Predicting the onset of rafting of γ' precipitates by channel deformation in a Ni superalloy

N. Ratel[a]*, H.A. Calderon[b], T. Mori[c] and P.J. Withers[c]

[a]*CIRIMAT ENSIACET, 31077 Toulouse cedex 4, France;* [b]*Departamento de Ciencia de Materiales, Instituto Politecnico Nacional, DF Mexico;* [c]*Materials Science Centre, University of Manchester, Manchester, M1 7HS, UK*

The growth or shrinkage, normal to {001}, of the interfaces between the γ matrix and cuboidal γ' precipitates is examined for a Ni-base superalloy, by considering the force acting on the interfaces. The force is produced by the precipitate coherency misfit and the stress produced by plastic deformation in channels of the γ matrix. A simple expression, which directly addresses the origin of the surface force, is given. The plastic deformation within the initially active γ matrix channels exerts the force to cause rafting. The subsequent activation of other types of channels also promotes the rafting in the same direction as the first active channels, when the plastic strain of the former channels increases. These issues are also discussed in terms of analysis based on those dislocations caused by the precipitate misfit and those produced by the plastic deformation.

Keywords: force on interface; γ-γ' alloy; channel deformation; rafting

1. Introduction

It is well known that Ni-base superalloys can exhibit rafting after creep deformation whereby the γ' precipitates, which are cuboidal before deformation, change to a flat shape. Rafting was also reported in specimens plastically deformed at a low temperature and subsequently annealed at a high temperature [1]. In this case plastic deformation occurs only in the γ matrix. This suggests that it is the internal stress produced by the matrix deformation combined with the stress field induced by the precipitate misfit strain that causes rafting. It is also recognized that plastic deformation occurs only in selected channels in the early stage of deformation [2,3]. When a single crystal is uniaxially loaded along [001], three types of matrix channels exist, namely those parallel to (001), (100) and (010). For example, when the precipitate misfit of γ' is negative as in most engineering γ-γ' alloys and the loading is tensile, only (001) channels (horizontal channels) are active plastically at the beginning of plastic deformation [4,5].

This observation suggests that rafting geometry should be discussed in conjunction with channel deformation. In fact, Socrate and Parks analyzed creep deformation by a finite element method and found channel deformation. They also

*Corresponding author. Email: nicolas.ratel@ensiacet.fr

calculated a force acting on the γ-γ' interface, using an energy-momentum tensor expression in order to examine the rafting geometry [6]. There are many other studies which have treated the case of rafting under uniaxial stress. The pioneering work of Pineau [7] treated the case of an isolated spherical particle in the frame of isotropic elasticity. This work was further extended to anisotropic elasticity and to the case of several particles with good accuracy [8]. Diffusion phenomena and cross-diffusional creep involved in rafting have been described previously [9]. In the latter, the calculations involved finite element analysis.

However, in the present paper, the application of an external stress is not considered. Instead, plastic deformation resulting from the application of an external stress is introduced in some matrix channels. This is because simple annealing under no external stress after prior plastic deformation also leads to rafting [1]. This experimental result is the starting point of the present study. Using an analytical approach based on an inclusion method and based on energy evaluation, we have confirmed the occurrence of channel deformation [10]. This requires the calculation of the internal stress developed by the specific channel type deformation. From this we can evaluate the force acting on γ-γ' interfaces analytically. Accordingly, the direction of the rafting geometry can also be inferred in a simple manner. The present study is intended to show these points.

Instead of the energy-momentum tensor, we will use a different expression to calculate the force on a γ-γ' interface. Of course the two methods are equivalent, but the present method is easier to use and can directly address the causes of the force, as shown later.

2. Analysis

The γ' precipitates have the precipitate misfit (stress-free strain)

$$\varepsilon_{ij}^{T} = \varepsilon_0 \delta_{ij}. \tag{1}$$

The present study examines the case of

$$\varepsilon_0 < 0, \tag{2}$$

even though the case of $\varepsilon_0 > 0$ can be dealt with in a similar manner, as briefly discussed later. It should be noted that the former case applies to most engineering Ni-base superalloys.

2.1. *Review of a previous analysis of stress*

It is assumed that the γ' particles are cuboidal, are nearly periodically arranged and are quasi-coherent with the γ matrix on $\{001\}$. It has been shown that when a tensile load is applied to [001], only the matrix channels, parallel to (001), undergo plastic deformation at the beginning of deformation [10]. This is because the interaction energy for plastic deformation within (001) channels with the precipitate misfit (2) is negative while that for plastic deformation within (100)/(010) channels is positive, when plastic strain of elongation occurs along [001].

In Figure 1(a), γ' particles and (001) and (100) channels are sketched out. It is important that the widths of the channels are far smaller than the size of the γ' particles, since we are examining a situation where the volume fraction of γ' can be as large as 0.7, the value in typical engineering Ni-base superalloys.

When a (001) channel plastically deforms by

$$\varepsilon_{33}^P = \varepsilon_P, \quad \varepsilon_{11}^P = \varepsilon_{22}^P = -\varepsilon_P/2, \quad (\varepsilon_P > 0) \tag{3}$$

the internal stresses in this channel are calculated as

$$\sigma_{11}^\infty = \sigma_{22}^\infty = \frac{(C_{11} + 2C_{12})(C_{11} - C_{12})}{2C_{11}}\varepsilon_P, \quad \sigma_{33}^\infty = 0, \text{ inside a channel} \tag{4}$$

as shown before [10]. Here, the x_1, x_2 and x_3 axes are taken along [100], [010] and [001], respectively. Eshelby's inclusion problem is used to calculate these stresses with the relevant tensors of $S_{3333} = 1$ and $S_{3311} = S_{3322} = C_{12}/C_{11}$. ($C_{11}$ and C_{12} are the relevant components of the elastic stiffness of a cubic material.) Here, a channel is approximated as a thin disk normal to [001]. The γ matrix and γ' precipitates are taken to have the same elastic constants for simplicity and without significant error. The investigations performed in [8] have shown that elastic misfit ceases to be important in the presence of plastic deformation. Since a channel is assumed flat, the stress corresponding to (4) vanishes outside the channel:

$$\sigma_{ij}^\infty = 0, \quad \text{outside a channel.} \tag{5}$$

When all the (001) channels are active, the plastic strain (3) also generates an average stress throughout the whole body, including (001) channels, the γ' particles and (100) and (010) matrix channels. This average stress is calculated as

$$\langle \sigma_{ij} \rangle = -F_3 \sigma_{ij}^\infty, \tag{6}$$

using the mean field method [12,13]. Here, F_3 is the volume fraction of the (001) channels. When the volume fraction of the γ' phase is 0.7 as proposed above, F_3 is

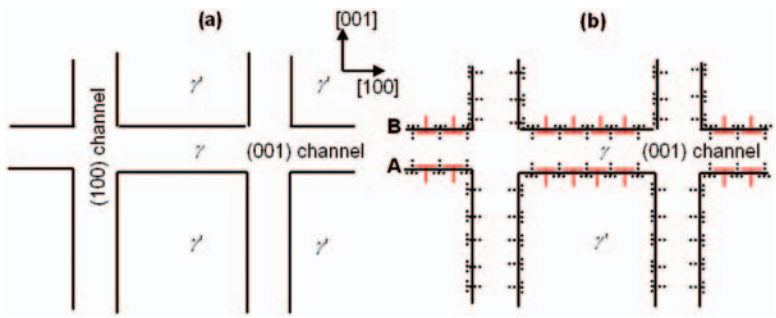

Figure 1. (a) Schematic arrangement of γ' particles and γ matrix channels. (b) Arrays of dislocations after plastic deformation in a (001) channel. An array of surface dislocations (shown by dotted line symbols) can be used to describe the γ-γ' misfit, while the plastic strain in a (001) channel can be thought of additional dislocations (shown by solid lines). These additional dislocations are produced by ε_{11}^P.

0.11 [10]. Thus, the stress σ_{ij}^{∞} due to a channel adjacent to a γ' particle is dominant over the average stress $\langle\sigma_{ij}\rangle$. Moreover, the average stress exerts the same force equally on all the $\{001\}$ γ-γ' interfaces of a γ' particle. This is partly due to the isotropic character of the precipitate misfit, (1). As seen later, the force is determined by the stress and the precipitate misfit. Thus, when the force on the γ-γ' interfaces is calculated to assess the direction of rafting, the effect of the average stress can be safely neglected.

2.2. *Force on γ-γ' interfaces due to plastic deformation in one type of matrix channels*

The standard formula to calculate a force on an interface is to use Eshelby's energy-momentum tensor

$$f = [\sigma_{ij}\varepsilon_{ij}]/2 - \sigma_{ij}[u_{i,j}]. \tag{7}$$

Although this form is different from that used by Socrate and Parks, the two expressions are equivalent [14]. Equation (7) is the form used by Su and Voorhees [15]; however, the expression given in [15] contained a typographical error which is corrected in the above. This force, per unit area, is normal to the interface and direct outwards to the outside of a precipitate. Here, σ_{ij} is the stress, ε_{ij} the elastic strain and $u_{i,j} = \partial u_i/\partial x_j$ is the total distortion. The square brackets mean the difference between the value just outside an interface and that just inside the interface. For example,

$$[u_{i,j}] = u_{i,j}(\text{out}) - u_{i,j}(\text{in}). \tag{8}$$

In the present study, instead, we will use the expression

$$f = \frac{\sigma_{ij}(\text{out}) + \sigma_{ij}(\text{in})}{2}\varepsilon_{ij}^{T}. \tag{9}$$

This equation is obtained by considering the virtual movement of an interface in the forward and backward directions. The forces defined by these virtual movements are averaged to give the above expression. The reason for the use of (9) is as follows: (i) Equation (9) gives the causes of the force directly: σ_{ij} is the action to cause the force on the boundary of a domain which is characterized by ε_{ij}^{T}. Together, these two factors indicate why the force exists. (ii) Equation (9) is similar to the Peach–Koehler force for a dislocation segment. The Peach–Koehler force contains the stress, the Burgers vector and tangential vector of the segment. (iii) If we are only concerned about the force due to the channel deformation, it is sufficient to use the stress of this origin in (9). The equivalence between (7) and (9) is demonstrated in the appendix.

Equation (9) is confidently applied with the condition that a γ-γ' interface is sharp. The analysis for the stress due to plastic deformation assumes that a deformed channel contacts an interface. Force is also evaluated by assuming the existence of a sharp interface, as seen later. Figure 2 provides support for this condition for all practical purposes. Figure 2 is a reconstructed high resolution (HREM) image of a Ni superalloy, containing a γ-γ' interface. With this condition, the γ' particles are quasi-coherent with the γ matrix and cuboidal. The γ' phase can be distinguished by the characteristic contrast arising from the chemical difference of the (200) planes in

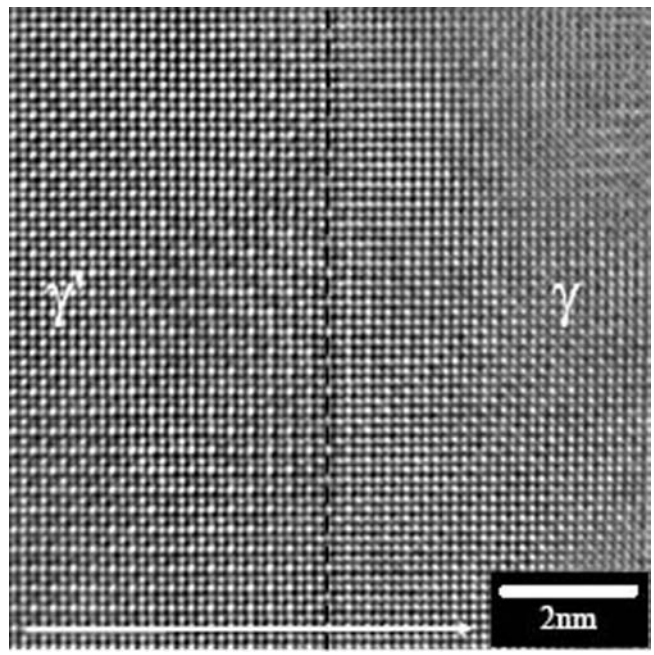

Figure 2. A high resolution reconstructed electron microscopy image of a Ni-12at%Al alloy containing a γ-γ' interface.

the $L1_2$ unit cell. The disordered γ phase lacks such a contrast variation. A γ-γ' interface is clearly seen in Figure 2. The contrast between the two phases changes sharply across the interface, indicating that the interface is sharp. Using the algorithm in *TrueImage* (REI) [16], and several images taken under different microscope settings, the true positions of the atomic columns can be obtained from the so-called exit wave reconstruction procedure. This makes possible an accurate measurement of the lattice spacings both perpendicular and parallel to the interface in Figure 2. When the spacings of the lattice planes parallel to the interface was measured across the interface, it was found that the spacing changed from the γ' to the γ phase within two unit cells [17]. The image in Figure 2 and this spacing measurement are believed to be convincing evidence for the sharpness of the γ-γ' interface.

2.3. *Force to initiate rafting due to plastic deformation in a (001) channel*

Only the difference in the force between the (001) and (100)/(010) interfaces plays a role in the rafting, as mentioned before. Thus, the average stress (6) can be omitted in discussing the onset of the rafting. Only (4) and (5) are required to calculate the force on a (001) γ-γ' interface. Using (9), (4) and (5), the force on a (001) interface of a γ' particle adjacent to a plastically deformed (001) channel is calculated as

$$f(001) = \frac{(C_{11} + 2C_{12})(C_{11} - C_{12})}{2C_{11}} \varepsilon_P \varepsilon_0. \tag{10}$$

Since

$$C_{11} > 0, \quad C_{11} + 2C_{12} > 0, \quad C_{11} - C_{12} > 0, \tag{11}$$

for thermodynamical reasons [18] and

$$\varepsilon_P \varepsilon_0 < 0 \tag{12}$$

under the present condition,

$$f(001) < 0. \tag{13}$$

This means that an originally cuboidal γ' particle tends to becomes thinner along [001], so that its eventual shape becomes flat parallel to (001). This is the correct rafting geometry observed [19].

2.4. *Role and effect of (100) or (010) channel deformation after initial straining in (001) channels*

After some straining in the (001) channels, (100)/(010) channels also start to deform plastically. This is because the internal stress of (6) with (4) promotes the lateral contraction of plastic strain in these channels. In other words, the interaction energy between (6) and the plastic strain in the (100)/(010) channels, the elongation of which occurs along [001], is negative.

The quantitative argument for this is as follows: After the strain of ε_P in the (001) channels, the elastic energy, per unit volume, is given as

$$E(001) = E_S(001) + E_I(001). \tag{14}$$

Here, $E_S(001)$ is the elastic self-energy due solely to the plastic strain in the (001) channels and $E_I(001)$ is the interaction energy between this plastic strain and the precipitate misfit. Using a standard method, these are calculated as [10]

$$E_S(001) = -(1/2)F_3(1 - F_3)\sigma_{ij}^{\infty}\varepsilon_{ij}^{P} = F_3(1 - F_3)\frac{(C_{11} + 2C_{12})(C_{11} - C_{12})}{4C_{11}}\varepsilon_P^2 \tag{15}$$

and

$$E_I(001) = -f(-F_3\sigma_{ij}^{\infty})\varepsilon_{ij}^{T} = fF_3\frac{(C_{11} + 2C_{12})(C_{11} - C_{12})}{C_{11}}\varepsilon_0\varepsilon_P, \tag{16}$$

where f is the volume fraction of the γ' particles.

Suppose that the (100) and (010) channels start to deform plastically after the above deformation. The plastic strain in the (100) channels is assumed to be

$$\varepsilon_{33}^{P'} = \varepsilon_P', \varepsilon_{11}^{P'} = -(1/2 - \alpha)\varepsilon_P', \quad \varepsilon_{22}^{P'} = -(1/2 + \alpha)\varepsilon_P', (\varepsilon_P' > 0). \tag{17}$$

Here, the parameter α is introduced to account for the large difference between the dimension along the [100] direction and that along the [010] direction of a (100) channel. However, this parameter must observe the condition

$$-1/2 \leq \alpha \leq 1/2. \tag{18}$$

The stress due to (17) in a (100) channel is calculated as [10]

$$\sigma_{11}^{\infty'} = 0, \quad \sigma_{22}^{\infty'} = \frac{C_{11} - C_{12}}{C_{11}}\{(C_{11} + C_{12})(1/2 + \alpha) - C_{12}\}\varepsilon_P', \\ \sigma_{33}^{\infty'} = -\frac{C_{11} - C_{12}}{C_{11}}\{-C_{12}(1/2 + \alpha) + C_{11} + C_{12}\}\varepsilon_P'. \tag{19}$$

Of course the corresponding stress outside one channel vanishes. The average stresses due to all the (100) channels are calculated similarly to (6), by replacing F_3 with the volume fraction of the (100) channels, $F_1(=F_3)$.

The (010) channels also deform plastically with the plastic strain of

$$\varepsilon_{33}^{P''} = \varepsilon_P', \varepsilon_{11}^{P''} = -(1/2 + \alpha)\varepsilon_P', \quad \varepsilon_{22}^{P''} = -(1/2 - \alpha)\varepsilon_P', \quad (\varepsilon_P' > 0) \tag{20}$$

from symmetry with (17). This strain results in the stress in one (010) channel being

$$\sigma_{22}^{\infty''} = 0, \quad \sigma_{11}^{\infty''} = \frac{C_{11} - C_{12}}{C_{11}}\{(C_{11} + C_{12})(1/2 + \alpha) - C_{12}\}\varepsilon_P', \\ \sigma_{33}^{\infty''} = -\frac{C_{11} - C_{12}}{C_{11}}\{-C_{12}(1/2 + \alpha) + C_{11} + C_{12}\}\varepsilon_P'. \tag{21}$$

The average stresses as due to the (010) channels are similarly written to the case of the (100) channels, using the volume fraction of these channels $F_2(=F_3 = F_1)$.

The elastic energy change due to the deformation of the (100) and (010) channels is

$$E(100/010) = E_S(100/010) + E_I(100/010) + E_I^P(001/100/010), \tag{22}$$

where $E_S(100/010)$ is the elastic self-energy due solely to the plastic deformation in the (100)/(010) channels, $E_I(100/010)$ is the interaction energy between the plastic strain in the (100)/(010) channels and the precipitate misfit and $E_I^P(001/100/010)$ is the interaction energy between all the channels. The first term, $E_S(100/010)$, is quadratic with respect to ε_P'

$$E_S(100/010) = B\varepsilon_P'^2, \tag{23}$$

where B is written in terms of F_1, F_2, C_{11}, C_{12} and α. Similar to $E_I(001)$, (16), the second and third terms in (22) are written as

$$E_I(100/010) = -f(-F_1\sigma_{ij}^{\infty'} - F_2\sigma_{ij}^{\infty''})\varepsilon_{ij}^T \\ = 2fF_1\frac{(C_{11} + 2C_{12})(C_{11} - C_{12})}{C_{11}}(\alpha - 1/2)\varepsilon_0\varepsilon_P' \tag{24}$$

and

$$E_I^P(001/100/010) = -F_1(-F_3\sigma_{ij}^{\infty}\varepsilon_{ij}^{P'} - F_3\sigma_{ij}^{\infty}\varepsilon_{ij}^{P''}) \\ = -F_3F_1\frac{(C_{11} + 2C_{12})(C_{11} - C_{12})}{C_{11}}\varepsilon_P\varepsilon_P'. \tag{25}$$

Since $\alpha \leq 1/2$ and $\varepsilon_0 < 0$, (24) is positive and thus the (100)/(010) channels do not plastically deform initially (i.e. when ε_P is small). However, (25) is negative and its magnitude exceeds (24) when ε_P becomes large. That is, the prior activity of the (001) channels promotes the occurrence of the plastic deformation in the (100)/(010) channels.

We can determine the plastic strain, ε_P, above which the (100)/(010) channels also participate in plastic deformation [11]. Instead, we just evaluate the force due to the plastic strains in the (100)/(010) channels in the following manner.

Using (9) and (19), the force due to a (100) channel deformation on a (100) interface is written as

$$f(100) = \frac{(C_{11} + 2C_{12})(C_{11} - C_{12})}{2C_{11}}(\alpha - 1/2)\varepsilon'_P\varepsilon_0. \tag{26}$$

The parameter α can be qualitatively estimated below. When ε'_P is small, $E_S(100/010)$ can be ignored compared to $E_I(100/010)$. $E_I^P(001/100/010)$ does not depend on α. Thus, the smallest increase in elastic energy, (22), due solely to the plastic strains in the (100)/(010) channels is attained when

$$\alpha = 1/2. \tag{27}$$

Accordingly, when the plastic strain ε'_P in the (100)/(010) channels is small

$$f(100) = 0, \tag{28}$$

so that there is no effect of the (100)/(010) channel deformation on the force, $f(100)$, on a (100) interface. By examining (19), (28) is found to be due to the fact that the force caused by $\sigma_{33}^{\infty'}$ and that caused by $\sigma_{22}^{\infty'}$ cancel out. There is a simple reason for $\alpha = 1/2$ and the cancelling result in $f(100) = 0$, as shown later in the Discussion. We can give the identical result for the force on (010), $f(010)$, using the stress $\sigma_{ij}^{\infty''}$.

It should be noted, however, that as the deformation progresses in the (100)/(010) channels, the elastic energy term of $E_S(100/010)$ increases. In this case α decreases so that the sum of $E_S(100/010)$ and $E_I(100/010)$ is minimized [10]. When this occurs, $f(100)$, for example, becomes positive. That is, in this stage, the (100)/(010) channel deformation promotes the shape change of the γ' particles in the same direction of rafting as was produced by the original (001) channel deformation. In other words, it accentuates the observed rafting.

2.5. *Cases of $\varepsilon_0 > 0$ or compression loading along [001]*

As seen above, the interaction energy determines whether (001) or (100)/(001) channels operate first when uniaxial loading is applied to [001]. The interaction energy is proportional to $\varepsilon_0 \times$ the plastic strain (elongation or compression). Depending on the sign of this product, we can easily determine the first acting channels. Also, the force on a particular interface is proportional to this factor. In this way, we can easily determine the rafting geometry without conducting detailed calculations.

We can also see the effect of the factor α easily. In the very beginning of the (100)/(010) channel deformation, $E_I(100/010)$ is more dominant over $E_S(100/010)$. Whether the (001) or (100)/(010) channels operate first, $E_I^P(001/100/010)$ does not depend on α. $E_I(100/010)$ is also proportional to the above factor. The proportional constant depends on α. Thus, we chose α which makes $E_I(100/010)$ smallest in the range of (18). It is noted that $E_I(100/010)$ has the same form as (24) for any combination of the precipitate misfit and plastic strain. Thus, when $\varepsilon_0\varepsilon'_P > 0$, we choose $\alpha = -1/2$ to examine the case at the very beginning of the (100)/(010) channel deformation.

3. Discussion

The result of the present study agrees, in terms of force on a γ-γ' interface, with that given by Socrate and Parks in an overall sense [6]. However, some differences should be recognized between the two studies. While Socrate and Parks predict the force numerically using finite elements, the present study gives the analytical expression of a force on an interface. It is believed that this analytical expression is more easily grasped and exploited. In addition, the present study has also examined the roles of (100)/(010) channels which becomes active after the prior activity of (001) channels. Our study is, in a sense, more realistic since our analysis is for 3D deformation, while Socrate and Parks employed a 2D analysis.

The FEM calculation employs a mesh producing procedure to describe a plastic channel. Thus, one might think that a FEM analysis is more detailed than the present study which assumes uniform plastic deformation in the channel. However, we have to recognize that an elementary process of plastic deformation in a channel is a dislocation movement. This movement leaves the trail of the dislocation on the γ-γ' interface. Its moving segment is curved. The radius of the curvature determines the stress to move it. This radius is half the width of the channel width in a simplified model. Once a stress exceeds a critical value determined by the width, the plastic deformation can occur throughout the channel. Thus, as long as an external stress is sufficiently large, we can envisage that a channel can deform relatively uniformly. Even if this argument is too strong, one must accept that the plastic strain is uniform along the width of a channel. Moreover, the present study offers the basic idea, with which the force on a γ-γ' can be examined under any combination of tensile or compressive loading and sign of the precipitate misfit without complex and time consuming recalculation. This is an advantage over a numerical method.

The force on a γ-γ' interface and the selection of plastic channels can be readily visualized when we take a dislocation view. The precipitate misfit induces the continuously distributed (surface) virtual dislocations on γ'-γ interfaces [21], as schematically shown by the dotted lines in Figure 1(b). On interface A, there are two types of these surface dislocations. One is due to ε_{11}^T and the other due to ε_{22}^T. Each type of dislocations results from the recombination at the interface of $a/2\langle 110\rangle$ gliding dislocations. The total Burgers vector of these dislocations, per unit area, are given as

$$\begin{aligned} \boldsymbol{B}_1 &= (\varepsilon_0, 0, 0) \quad \text{for dislocations parallel to [010]}, \\ \boldsymbol{B}_2 &= (0, \varepsilon_0, 0) \quad \text{for dislocations parallel to [100]}. \end{aligned} \tag{29}$$

These are of edge type. The dotted lines for A in Figure 1(b) is for $\boldsymbol{B}_1$.

The plastic deformation (3) in a (001) channel leaves dislocations shown schematically by the solid lines in Figure 1(b). These dislocations are due to the component of ε_{11}^P. Even though the actual plastic deformation of this multiple slip (3) occurs by the movement of glide dislocations having many types of the Burgers vectors, the resultant product of these dislocations on a γ-γ' interface can be simplified as depicted in Figure 1(b). Using the Peach–Koehler expression of a force on a dislocation, the force on the surface dislocations A can be calculated as

$$f_{\text{disl}} = \frac{(C_{11} + 2C_{12})(C_{11} - C_{12})}{2C_{11}} \varepsilon_0 \varepsilon_P, \tag{30}$$

which directs along [001]. This agrees with $f(001)$, (10). Here, (4) and (5) are used to calculate the principal values of the stresses. The stresses due to (3) jump across interface A. In such a case, the stresses to be used for the Peach–Koehler expression are the principal value, as shown by Brown [22] and used to examine thermal stress relief from a second phase particle [23].

Figure 1(b) also shows why the plastic strain (3) in a (001) channel occurs first when $\varepsilon_0 < 0$. The dislocations generated by this strain cancel out the stress due to the dislocations representing the precipitate misfit. The Burgers vectors of the two types of dislocations, solid lines and dotted lines, on a (001) interface have opposite signs.

It is also noted that the force on the virtual dislocations (dotted lines) on interface A is not caused by those dislocations (solid lines) on the same interface. This is because the principal values of the stress of the glide (latter) dislocations vanish on the interface. There is another way to see this point. Let interface A in Figure 1(b) move downwards virtually. Since the Burgers vectors of the dotted line and solid line dislocations have different signs, the solid line dislocations exert an attractive force on the dotted line dislocations on the displaced γ-γ' interface. This force tends to restore the interface into its original position. The same result is obtained when the interface virtually moves upwards. In brief, the solid line dislocations exert no net force on the dotted line dislocations on the same interface A. On the contrary, the solid line dislocations on interface B have the same sign in the Burgers vector as the dotted line dislocations on interface A. Thus the force between these two arrays of dislocations is always repulsive. In this way we can understand that the force for the movement of interface A is caused by the dislocations (solid lines) on interface B.

As discussed in Section 2.4, the plastic deformation also occurs, for example, in a (100) channel after some strain in the (001) channels. The (100) channel strain $\varepsilon_{33}^{P'}$ leaves dislocations on the (100) interfaces as shown by the solid line dislocations in Figure 3(a), where the dislocations due to prior plastic deformation in a (001) channel are also shown. These are the same as those shown in Figure 1(b). The solid dislocations in array C have a Burgers vector of the same sign as the virtual dislocations due to the precipitate misfit (dotted line). Thus, the virtual dislocations representing the γ-γ' misfit repel those due to plastic deformation. This is the basic reason why (100)/(010) channels are not active at the beginning. To activate these channels, the internal stress due to the plastic deformation in (001) channels must increase.

When a (100) channel is viewed from the top along [001], we can draw Figure 3(b). The solid dislocations due to plastic deformation are caused by $\varepsilon_{22}^{P'}$. As seen in Figure 3(b), the stress field of the solid dislocations cancel that due to the dotted dislocations. This effect is most effective when the magnitude of $\varepsilon_{22}^{P'}$ is largest, equal to $-\varepsilon_{33}^{P'}$. This is the case of $\alpha = 1/2$ as analytically found in Section 2.4. See (17).

Figure 3(a) also shows that the (100) force due to the solid dislocations in array C and D is positive, while that due to the solid dislocations in arrays E and F in Figure 3(b) is negative when $\alpha = 1/2$; these forces cancel out exactly. This is why $f(100) = 0$ at the beginning of the operation of the (100) channels (the case of $\alpha = 1/2$).

Lastly, we will discuss what occurs after the inward movement of (001) interfaces, the movement which leads to rafting. To simplify the discussion, we consider the case that only the (001) channels operate. When the (001) interfaces move inwards, the lattice glide dislocations follow this movement and the width (volume fraction) of the

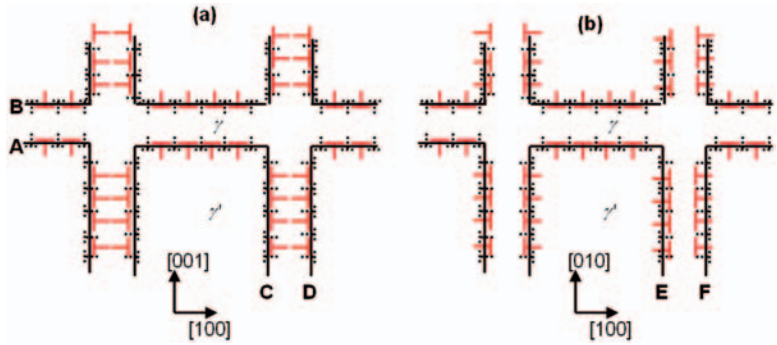

Figure 3. (a) Arrays C and D of dislocations (solid lines) are introduced by plastic deformation of $\varepsilon_{33}^{P'}$ in a (100) channel following prior plastic deformation in a (001) channel (shown in Figure 1b). (b) The top view along [001] of the (100) channel. Arrays E and F of solid dislocations are due to $\varepsilon_{22}^{P'}$.

(001) channels increases, as long as ε_P is below a certain magnitude. An energy decrease occurs in this process. Suppose that the volume fraction of the (001) channels increases by δF_3. This causes the energy change $\delta E_S(001)$ given by

$$\delta E_S(001) = \frac{(C_{11}+2C_{12})(C_{11}-C_{12})}{4C_{11}}\{(1-2F_3)\varepsilon_P + 4f\varepsilon_0\}\varepsilon_P \delta F_3. \tag{31}$$

Here, (14), (15) and (16) are used. If

$$(1-2F_3)\varepsilon_P < -4f\varepsilon_0, \tag{32}$$

$\delta E(001)$ is negative for an increase (δF_3) in F_3. That is, the expansion of the (001) channel width occurs. The above certain value of ε_P is

$$\varepsilon_P = -\frac{4f}{1-2F_3}\varepsilon_0. \tag{33}$$

As this process occurs, F_3 increases and eventually reaches the maximum value of $1-f$. When $f=0.7$, the above strain is $-7\varepsilon_0$. In the above, we ignored a change in the elastic energy attributed solely to the precipitate misfit. When the volume fraction of the (001) channels becomes maximum (0.3), the γ' precipitates take a flat shape parallel to (001). As shown before [10], this shape of the γ' precipitates makes the elastic energy due to the precipitate misfit lowest. Thus, the discussion for a change due to the volume increase of the (001) channels still holds.

The inward movement of the (001) interfaces is due to the diffusion of the constituent atoms, which can generate additional plastic deformation associated with cross-diffusion [9]. The expansion of the plastic channels is due to the movement of lattice glide dislocations. This movement does not require diffusion. It can occur by glide motion, as in the case of the formation of the arrays of the solid dislocations in Figures 1 and 3 due to original plastic deformation. Taking the contribution of diffusional processes into account would require significant additional numerical calculations, which are avoided in the present approach.

4. Summary

The start of rafting of γ' particles, as would occur at elevated temperature after room temperature plastic straining along [001], is due to internal stress caused by matrix plastic deformation. First, a simple expression for the surface force acting on a precipitate/matrix interface due to the precipitate misfit and the stress on the interface is presented. The type of γ matrix channels which undergo plastic deformation is determined by the sign of the precipitate misfit, from which the internal stress can be calculated. Using this stress, the force on a γ-γ' interface is expressed analytically and is found to change the shape of a γ' particle as described by rafting. The role of the subsequent activity of other types of channels after the deformation in the first type of channels is also evaluated. It is shown that the activity of the secondary channels either has no effect on the interface force for rafting or promotes the rafting. The surface force is generalized for any combination of the precipitate misfit and mode of loading to induce plastic deformation. The selection of active plastic deformation channels and the origin of the interface force are visualized by a dislocation analysis for the precipitate misfit and plastic deformation.

Acknowledgement

T. Mori acknowledges visiting fellowship funding from an EPSRC platform grant.

References

[1] M. Veron, Y. Brechet and F. Louchet, Scripta Mat. 34 (1996) p.1883.
[2] M. Feller-Kniepmeir and T. Link, Mat. Sci. Eng. A 113 (1989) p.191.
[3] T. Ichitsubo and K. Tanaka, Acta Mat. 53 (2005) p.4497.
[4] H.A. Khun, H. Biermann, T. Ugar and H. Mughrabi, Acta Met. Mat. 39 (1991) p.2783.
[5] T.M. Pollock and A. Argon, Acta Met. Mat. 42 (1994) p.1859.
[6] S. Socrate and D.M. Parks, Acta Met. Mat. 41 (1993) p.2185.
[7] A. Pineau, Acta Metall. Mater. 24 (1976) p.559.
[8] F.R.N. Nabarro, C.M. Cress and P. Kotschy, Acta Mater. 44 (1996) p.3189.
[9] F. Louchet and A. Hazotte, Scipta Mater 37 (1997) p.589.
[10] N. Ratel, P. Bastie, T. Mori and P.J. Withers, Mat. Sci. Eng. A 505 (2009) p.41.
[11] N. Ratel, M. Kawauchi, T. Mori, I. Saiki, P.J. Withers and T. Iwakuma, submitted to Mechanics of Materials (2009).
[12] L.M. Brown, Acta Metall. 21 (1973) p.879.
[13] T. Mori and K. Tanaka, Acta Metall. 21 (1973) p.571.
[14] T. Mura, *Micromechanics of Defects in Solids*, Martinus Nijhoff, 1982, p.314.
[15] C.S. Su and P.W. Voorhees, Acta Mater. 44 (1996) p.1987.
[16] W.M.J Coene, A. Thust, M. Op de Beeck and D. Van Dick, Ultramicroscopy 64 (1996) p.109.
[17] H. Calderon, in preparation.
[18] H.B. Callen, *Thermodynamics*, John Wiley, New York, 1960, p.231.
[19] M. Veron, Y. Brechet and F. Louchet, Scripta Met. 34 (1996) p.3189.
[20] N. Ratel, G. Bruno, P. Bastie and T. Mori, Acta Mater. 54 (2006) p.5087.
[21] T. Mura, *Micromechanics of Defects in Solids*, Martinus Nijhoff, 1982, p.341.
[22] L.M. Brown, Phil. Mag. 10 (1964) p.441.
[23] S. Shibata, M. Taya, T. Mori and T. Mura, Acta Met. Mat. 40 (1992) p.3141.

Appendix

Here, the general case that the eigenstrain ε_{ij}^{*} exists only inside a domain V is discussed. The equivalence between

$$f = (1/2)(\sigma_{ij}(\text{out})\varepsilon_{ij}(\text{out}) - \sigma_{ij}(\text{in})\varepsilon_{ij}(\text{in})) - \sigma_{ij}(u_{i,j}(\text{out}) - u_{i,j}(\text{in})) \tag{34}$$

and

$$f = \frac{\sigma_{ij}(\text{out}) + \sigma_{ij}(\text{in})}{2}\varepsilon_{ij}^{*} \tag{35}$$

is shown. Since σ_{ij} in (34) can be either $\sigma_{ij}(\text{out})$ or $\sigma_{ij}(\text{in})$, the second term in (34) is rewritten as

$$-\sigma_{ij}(u_{i,j}(\text{out}) - u_{i,j}(\text{in})) = -(1/2)(\sigma_{ij}(\text{out}) + \sigma_{ij}(\text{in}))(u_{i,j}(\text{out}) - u_{i,j}(\text{in})). \tag{36}$$

Noting that $\sigma_{ij}(u_{i,j} + u_{j,i})/2 = \sigma_{ij}u_{i,j}$ and

$$(u_{i,j}(\text{in}) + u_{j,i}(\text{in}))/2 = \varepsilon_{ij}(\text{in}) + \varepsilon_{ij}^{*}, \tag{37}$$

(36) is changed to

$$\begin{aligned} -\sigma_{ij}(u_{i,j}(\text{out}) - u_{i,j}(\text{in})) = &-(1/2)(\sigma_{ij}(\text{out})\varepsilon_{ij}(\text{out}) - \sigma_{ij}(\text{in})\varepsilon_{ij}(\text{in})) \\ &+ (1/2)\sigma_{ij}(\text{out})\varepsilon_{ij}(\text{in}) - (1/2)\sigma_{ij}(\text{in})\varepsilon_{ij}(\text{out}) \\ &+ (1/2)(\sigma_{ij}(\text{in}) + \sigma_{ij}(\text{out}))\varepsilon_{ij}^{*}. \end{aligned} \tag{38}$$

Inserting this into (34), we have

$$f = (1/2)\sigma_{ij}(\text{out})\varepsilon_{ij}(\text{in}) - (1/2)\sigma_{ij}(\text{in})\varepsilon_{ij}(\text{out}) + (1/2)(\sigma_{ij}(\text{in}) + \sigma_{ij}(\text{out}))\varepsilon_{ij}^{*}. \tag{39}$$

Since

$$\sigma_{ij}(\text{out})\varepsilon_{ij}(\text{in}) = \sigma_{ij}(\text{in})\varepsilon_{ij}(\text{out}), \tag{40}$$

the first two terms in (39) cancel. Thus, we have

$$f = (1/2)(\sigma_{ij}(\text{in}) + \sigma_{ij}(\text{out}))\varepsilon_{ij}^{*}, \tag{41}$$

which is identical to (35).

It is noted that $(\sigma_{ij}(\text{in})) + \sigma_{ij}(\text{out})))/2$ is the principal value of the stress which, in general, jumps across the interface of V. In the present analysis, the stress used to calculate the force on a γ-γ' interface is that due to plastic deformation occurring only in the gamma matrix. Due to the plastic deformation geometry considered, this stress is discontinuous across the interface. That is, $\sigma_{ij}(\text{in})$ is not equal to $\sigma_{ij}(\text{out})$. Thus, the average of these terms is crucial to evaluate the force on the interface. It is recalled that for a curved dislocation segment a similar averaged value of stresses is used [22] when the Peach–Koehler force due to the self stress is calculated. The self-stress of a curved dislocation is also discontinuous across the core of the segment.